



11th International Congress on Metallurgy & Materials SAM/CONAMET 2011.

Study of directional solidification of Zn-Al alloys

M. Pizarro Pastene^a, O. Fornaro^{b,c,*}, H. Ochoa Medina^a

a) Departamento de Ingeniería Mecánica, Universidad de Antofagasta, Av. Angamos 601, Antofagasta, Chile

b) Instituto de Física de Materiales Tandil (IFIMAT)

Universidad Nacional del Centro de la Provincia de Buenos Aires, Pinto 399, B7000GHG Tandil, Argentina

c) Consejo Nacional de Investigaciones Científicas y Técnicas (CONICET)

Abstract

Directional growth of Zn-Al alloys of different concentration was carried out by using a Bridgmann like apparatus. The compositions of studied systems were a) dilute Zn-0,5 wt.%Al, below the maximum solubility limit, b) hypo-eutectic Zn-2 and 4 %wt. Al, and c) hyper-eutectic Zn-8wt.% Al. Proper metallographic analysis of the segregation patterns behind the solid-liquid (S-L) interface gives information about the effect of the local solidification conditions to obtain different microstructures. It was found that the dilute alloy grows in a similar fashion than other alloys with atomistically rough interfaces. For alloys with composition above the maximum solubility limit, it was found that a single primary phase grows surrounded by liquid eutectic. In the case of hypo-eutectic alloys, a dendritic hcp primary phase is formed, whilst for hyper-eutectic alloys, the primary phase is an fcc Al-rich dendrite. In both cases, a secondary interface for eutectic solid-liquid is formed below the dendrite tips, in such a way the eutectic seems to growth independently of the primary phase.

© 2012 Published by Elsevier Ltd. Selection and/or peer-review under responsibility of SAM/CONAMET 2011, Rosario, Argentina. Open access under [CC BY-NC-ND license](https://creativecommons.org/licenses/by-nc-nd/4.0/).

Keywords: ZnAl alloys; Direccional solidification; microstructure

* Corresponding author. Tel.: +54-2293-439670; fax: +54-2293-439679.
E-mail address: ofornaro@exa.unicen.edu.ar.

1. Introduction

The microstructure formation during directional solidification of dilute alloys is a very important process, both from the academic point of view as for technological applications. For a recent review, it can be seen Boettinger et al., 2000. The Morphological Stability Theory (Sekerka, 1984; Coriell et al., 1990; Coriell and McFadden, 1993) defines several conditions under which an initially planar solid-liquid interface could become unstable and therefore form different microstructures.

Directional solidification by Bridgman method is a traditionally used tool to study the solidification of metallic alloys due to it permits the control of the thermal gradient, the growth rate of the solid-liquid interface and the chemical composition of the sample to be grown. Even though the evolution of the microstructure as a function of these variables has been widely studied in many metallic and transparent systems, such relationship is firstly qualitatively known in complex systems, where the anisotropy could play a significant role even in the low velocity regime. During the development of dendritic growth, the anisotropy of the surface energy allows to define a unique dendrite operative state, by fixating the relation between tip radius and primary spacing (Boettinger et al., 2000; Aziz, 1982; Biloni and Boettinger, 1996). Also, this anisotropy takes a fundamental role during the formation of the cellular growth (Fornaro and Palacio, 2006).

Numerous works have been developed to systematically study the solidification process, fundamentally in face centered cubic (fcc) crystallography dilute alloys. From them, it is possible to define different morphologies (Biloni and Boettinger, 1996; Fornaro et al., 2004; 2006) as a function of solidification parameters: G_L , thermal gradient at liquid; V , growth rate; C_0 , nominal composition of the alloy. For alloys with more complex crystallography, the morphology obtained during directional solidification may show a different behaviour depending on growth direction. A precise description of microstructural evolution does not exist for hexagonal closed packed (hcp) alloys and only some descriptions appear in the literature (Biloni et al., 1967; Audero and Biloni, 1972; 1973; Biloni and Boettinger, 1996; Fornaro and Palacio, 2006). In a recent work, the dependance of critical velocity and wavelength during planar to cellular transition with the direction of growth was demonstrated for hcp crystals (Fornaro and Palacio, 2006). The ZnAl alloy family has many technological applications, mainly close to the eutectic composition of Zn-5wt.%Al fundamentally by its singular behavior under corrosive environments.

In this work, the solidification of Zn-Al alloys by directional growth of a) hypo-eutectic composition (Zn-0,5 wt.%Al) below the maximum solubility limit, b) above such limit (Zn-2 and 4 wt.%Al), and c) a hyper-eutectic composition (Zn-8 wt.%Al) is studied, with the purpose of understanding the formation of the microstructures under different solidification paths, and then different primary phases.

2. Experimental

Directional growth of the samples was carried out in a Bridgman device. The details of the experimental device, the control of solidification parameters G_L and V , and the procedure applied to sample quenching were previously published (Fornaro and Palacio, 1994; 1997; Fornaro et al., 2004; 2006). A schematics of the device is shown in Fig. 1. The alloy was prepared starting from Zn (99.999%) and Al (99.99%) purity materials, carrying out the melting process in a SiC crucible which was painted internally with an alumina coating. Firstly, an eutectic alloy was obtained to be used as mother alloy. The eutectic composition of Zn-5%Al has a melting temperature of approximately 370 °C. This composition was obtained by melting appropriate quantities of Zn and Al under the mentioned conditions. The alloys with chemical composition below the eutectic, Zn-0.5, 2, and 4wt%Al, were obtained by melting Zn and the appropriate quantity of the eutectic alloy, previously obtained. Hiper-eutectic composition Zn-8wt.% Al was achieved by starting with

the eutectic mother alloy and adding Al to the melt. Cylindrical samples were obtained by conventional casting into graphite molds, and then machined to obtain 8 mm cylindrical samples to be directionally grown.

The samples partially grown were quenched by dropping the quartz tube into cold water. After that, samples are sectioned in transversal and longitudinal direction respect to the growth direction. The surface set up for optical microscopy observation and analysis requires great attention, because this alloy can show plastic deformation during the mechanical polishing, driving to twinning formation and the re-precipitation of small grains on the surface. To avoid these effects, an extremely slow and continuously refrigerated mechanical polishing was made, up to 600 grit SiC abrasive paper, refrigerated with water, and then with a supersaturated solution of alumina powder in water on a soft cloth. Electrolytic polishing was used, using a butoxi-ethanol + 10% glicerine + 10% perchloric acid electrolyte, with variable conditions. The Electro-polishing process generates a thick surface oxide which allows to detect changes in crystallographic orientation, when observed under polarized light in optical microscope.

3. Directional solidification

3.1. Zn-0.5wt.%Al

Directional solidification of small samples was carried out by using a Bridgman apparatus, fixing the thermal gradient at $G=2.5$ K/mm. This alloy has a composition below the maximum solubility limit for aluminum in Zn. As a result, a single phase could be obtained if the growth velocity is kept under the critical limit imposed by constitutional supercooling (Fornaro et al., 2006; Fornaro and Palacio, 2006)

$$\frac{G_L}{VC_0} = \frac{m_L}{D_L} \frac{(k_0 - 1)}{k_0} \quad (1)$$

In this equation, m_L is the slope of the liquidus line from the phase diagram of the alloy, D_L is the liquid solute diffusion constant and k_0 is the partition coefficient under equilibrium conditions. The calculated value for this critical condition is $V_C = 0.6$ $\mu\text{m/s}$. For greater values of velocity under this thermal gradient, cellular or dendritic morphology could be obtained. For example, Fig 1a) shows the typical quenched interface, showing a cellular microstructure. In the figure the growth is developed in the upright direction. In Fig. 1b) and c) it can be seen transversal views for different growth velocities. As seen, the intercellular spacing shows a higher Al concentration, despite there is no evidence of eutectic composition on the cellular wall. In other systems like dilute Al-Cu alloys, it was demonstrated that the second phase could be present even at very low solute concentrations, but the expected $\alpha + \theta$ eutectic structure is not formed (Fornaro et al., 2006). This could be the case for alloy with solute concentrations below the solubility limit. Also the dissolution of the second

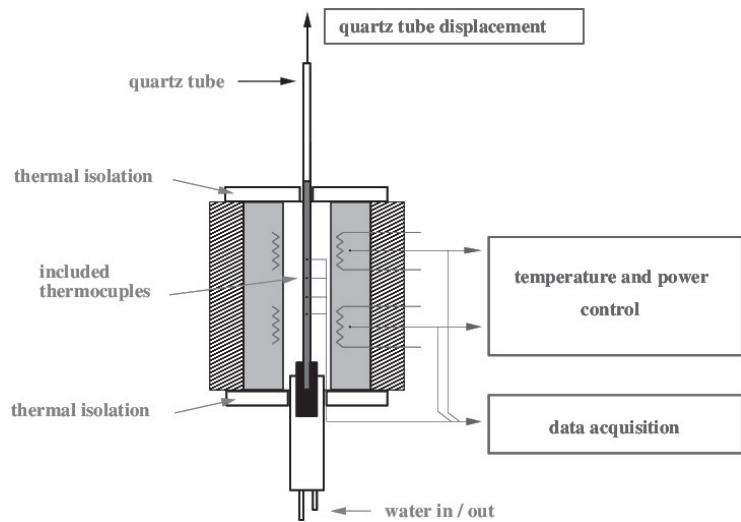


Figure 1: Schematics of the growth device.

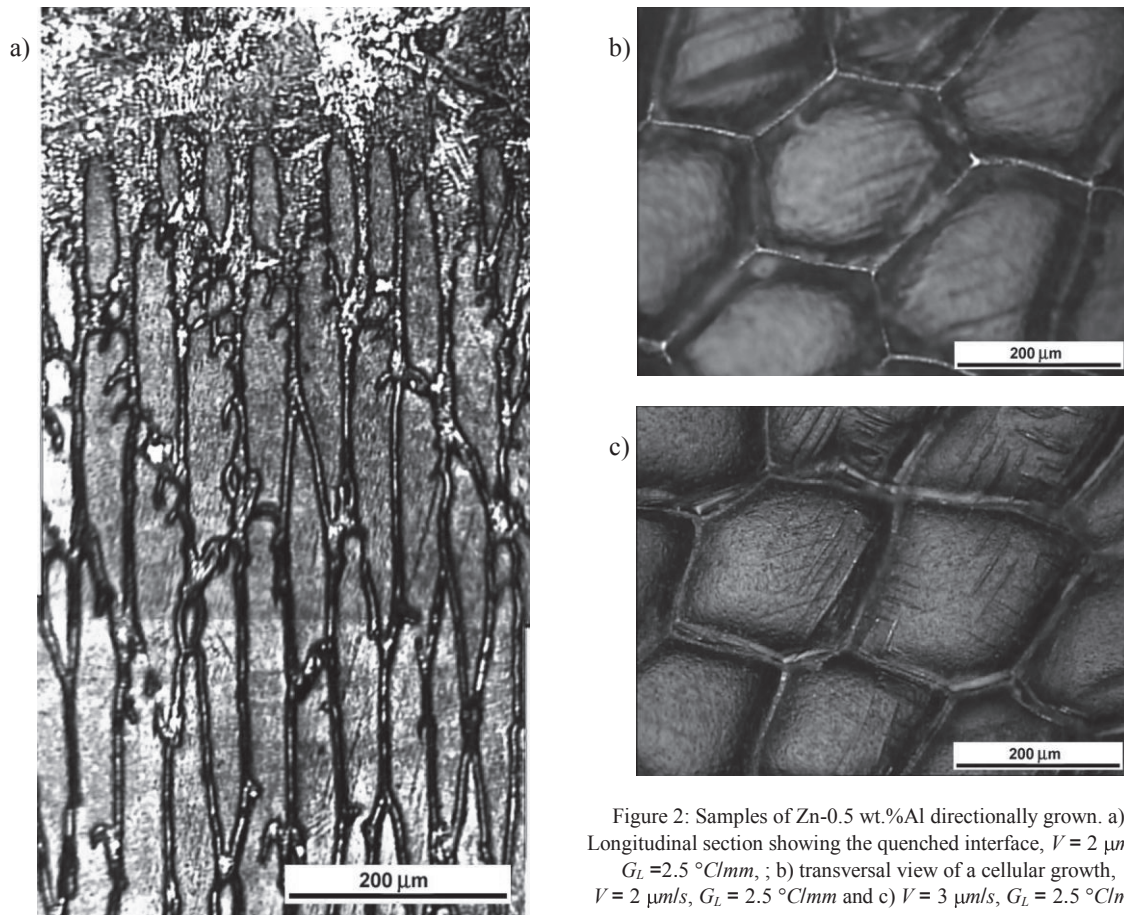


Figure 2: Samples of Zn-0.5 wt.%Al directionally grown. a) Longitudinal section showing the quenched interface, $V = 2 \mu\text{m/s}$, $G_L = 2.5 \text{ }^\circ\text{C/mm}$; b) transversal view of a cellular growth, $V = 2 \mu\text{m/s}$, $G_L = 2.5 \text{ }^\circ\text{C/mm}$ and c) $V = 3 \mu\text{m/s}$, $G_L = 2.5 \text{ }^\circ\text{C/mm}$

phase is observed on long samples, because the sample remains at high temperature during the directional growth, long enough to induce the phase dissolution.

3.2. Zn-2 and 4wt.%Al

Samples directionally grown with composition greater than 1.25 wt.%Al, show typical cellular and dendritic morphology. The expected theoretical value of critical velocity for planar to cellular transition under a thermal gradient of $G_L = 2,5 \text{ K/mm}$ is $V_C = 0.15 \mu\text{m/s}$. Even when the composition is below the eutectic composition, the solidification must begin with a primary phase finishing with the solidification of trapped liquid of eutectic concentration. This means that a two-phase morphology must appear at the interdendritic space. This behavior is shown in Fig. 3 for Zn-2 wt.%Al. Fig. 3 a) shows the longitudinal section of a sample. At this magnification, the microstructure at the intercellular cannot be resolved. However, the higher magnification of Fig. 3 b) and c) clearly show two different phases. The situation for Zn-4 wt.%Al is similar, but it can be observed in Fig. 4 that the amount of eutectic is greater than in the previous case, as can be expected by applying the lever rule. Fig. 4a) and b) show a longitudinal view of a quenched solid-liquid obtained under $G_L = 2.5 \text{ K/mm}$ and $V = 1.5 \mu\text{m/s}$. In these figures it appears that the intercellular liquid

eutectic is growing by forming a two phase solid, without apparent interaction with the neighboring dendritic cells.

3.3. Zn-8wt.%Al

Samples of Zn-8 wt.%Al were directionally grown in a similar way than Zn-4wt.% Al, but in this case primary dendrites of f.c.c. aluminum rich phase are projected into the liquid. Fig. 5a) shows a longitudinal view of a sample grown at $G_L=2.5$ K/mm and $V=1.5$ $\mu\text{m/s}$, showing a dendritic growth with a great amount of interdendritic liquid. As in the previous case, an eutectic-liquid interface is formed below the solid-liquid interface corresponding to the dendrite tip imaginary line. A detailed view of the situation is shown in Fig. 5b). The central part of the figure shows the interdendritic region where the quenched eutectic-liquid interface surrounded by the solid aluminum-rich primary phase can be noted.

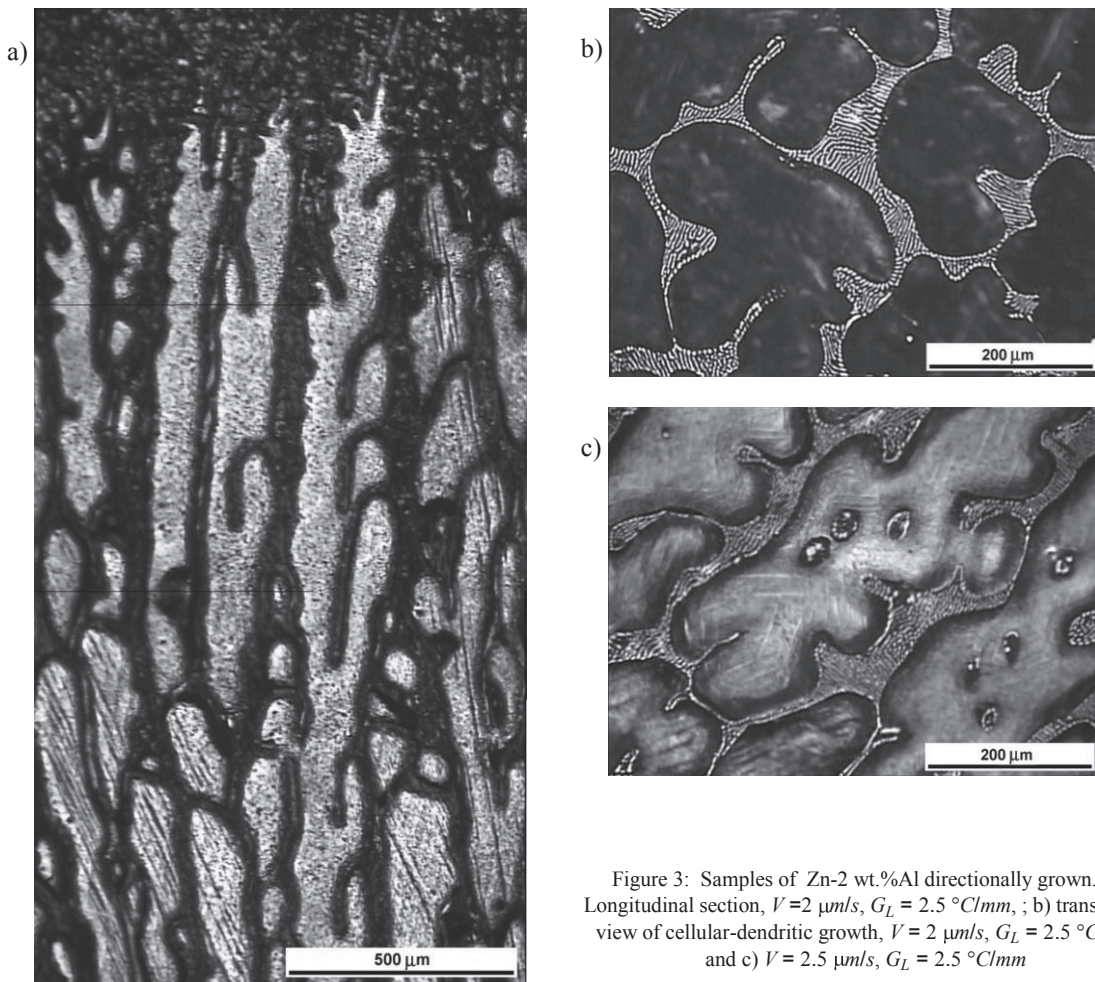


Figure 3: Samples of Zn-2 wt.%Al directionally grown. a) Longitudinal section, $V=2$ $\mu\text{m/s}$, $G_L = 2.5$ $^\circ\text{C/mm}$; b) transversal view of cellular-dendritic growth, $V = 2$ $\mu\text{m/s}$, $G_L = 2.5$ $^\circ\text{C/mm}$ and c) $V = 2.5$ $\mu\text{m/s}$, $G_L = 2.5$ $^\circ\text{C/mm}$

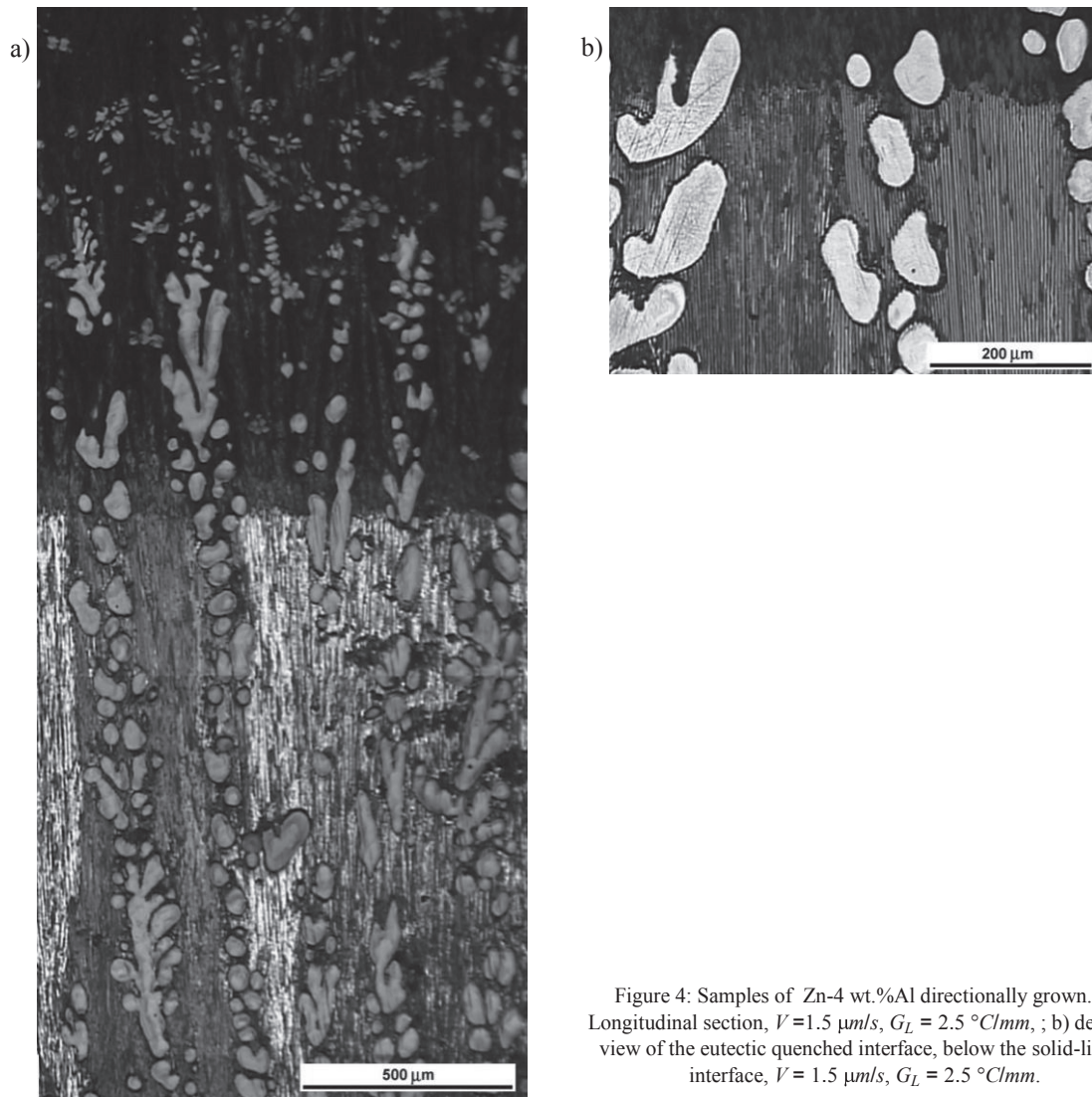
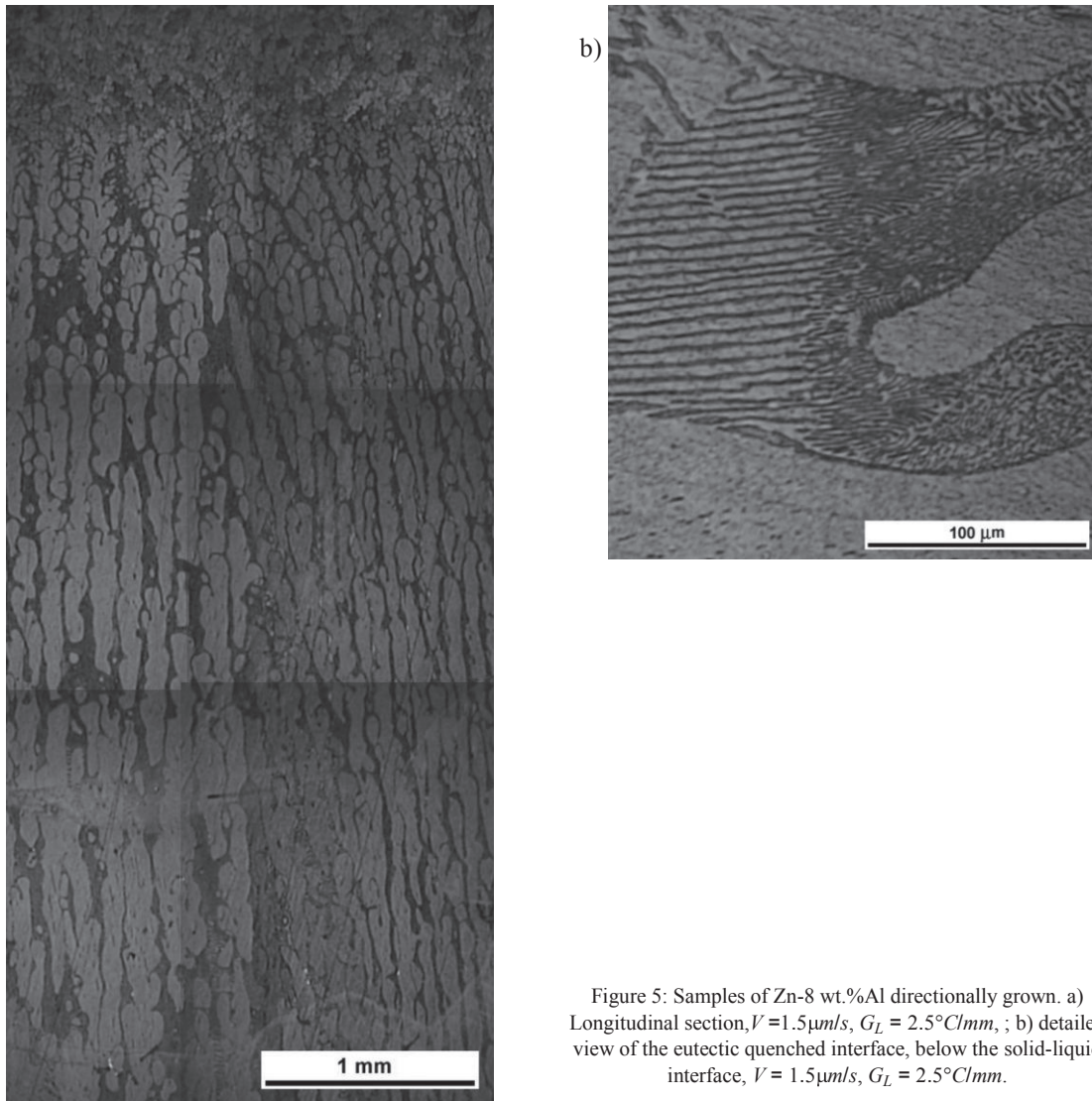


Figure 4: Samples of Zn-4 wt.%Al directionally grown. a) Longitudinal section, $V=1.5 \mu\text{m/s}$, $G_L = 2.5 \text{ }^\circ\text{C/mm}$, ; b) detailed view of the eutectic quenched interface, below the solid-liquid interface, $V = 1.5 \mu\text{m/s}$, $G_L = 2.5 \text{ }^\circ\text{C/mm}$.

3.4. Solidification model

A solidification schema is depicted in Fig. 6 where a primary interface is formed for the line of dendrite tips and liquid, in such a way that these dendritic cells are trapping solute rich liquid that can solidify at adequate temperature forming a second eutectic-liquid interface. As shown in figures 4 and 5 the eutectic growth is columnar, and apparently independent of the dendrites around, at least as long as it has enough space to grow. Dendrites of primary phase are growing as independent dendritic cells toward an undercooled liquid.



4. Conclusions

Samples of dilute Zn-0.5 wt.%Al, pro-eutectic Zn-2 and 4 wt.%Al and hyper-eutectic Zn-8 wt.%Al were directionally grown.

Directionally grown Zn-0.5 wt.%Al shows cellular and dendritic cell morphology within the studied velocity range. Samples with pro-eutectic composition show a dendritic primary phase, surrounded by eutectic, growing without apparent interaction. Greater solute concentrations results in a greater amount of eutectic, as can be explained by using a simple lever rule analysis. Hyper-eutectic alloys grown in a similar way as pro-eutectic, unless primary phase in this case is an f.c.c. aluminum rich phase.

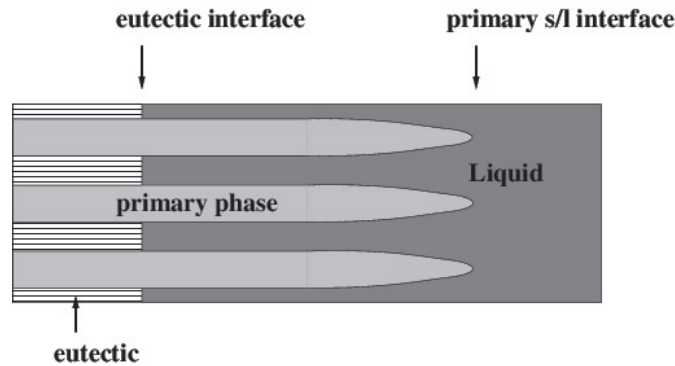


Figure 6: Idealization of the solidification mechanism for chemical compositions larger than the maximum solubility limit, and around the eutectic composition

In all the cases, the expected phases can be predicted by the solidification path which can be theoretically calculated or found by a cooling curve analysis.

Acknowledgements

This work was carried out at the IFIMAT (Instituto de Física de Materiales Tandil) and has been partially supported by CICPBA (Comisión de Investigaciones Científicas de la Provincia de Buenos Aires), CONICET (Consejo Nacional de Investigaciones Científicas y Técnicas) and SeCAT-UNCPBA (Secretaría de Ciencia, Arte y Tecnología de la Universidad Nacional del Centro de la Provincia de Buenos Aires).

References

- Audero, M. A.; Biloni, H.; 1972, The dendritic morphology in Zn-Cd dilute alloys, *Journal of Crystal Growth*, 12, p 297.
- Audero, M. A.; Biloni, H.; 1973, The development of cells during the solidification of dilute Zn-Sn alloys, *Journal of Crystal Growth* 18, p 257.
- Aziz M. J., 1982, Model for Solute Redistribution During Rapid Solidification, *Journal of Applied Physics*, **53**, p1158.
- Biloni, H.; di Bella, R. & Bolling, G. F., 1967, On microsegregation nodes and cellular solidification substructures in dilute tin alloys, *Trans. Met. Soc. AIME*, 239, p 2012.
- Biloni, H., Boettinger, W. J., 1996, Ch. 9, Solidification in *Physical Metallurgy*, Vol. II, R. W. Cahn and P. Haasen. eds. Elsevier Science Publishers, p 669.
- Boettinger, W. J.; Coriell, S. R.; Greer, A. L.; Karma, A.; Kurz, W.; Rappaz, M.; Trivedi, R., 2000, Solidification microstructures: recent developments, future directions, *Acta Materialia*, 48, p 43.
- Coriell, S. R., McFadden, G. B., 1993, Morphological Stability in *Handbook of Crystal Growth*. D. T. J. Hurle ed. Elsevier Science Publishers, Vol. 1B, p 785.
- Coriell, S.; McFadden, G., Sekerka, R., 1990, Effect of anisotropic thermal conductivity on the morphological stability of a binary alloy, *Journal of Crystal Growth*, 100, p 459.
- Fornaro, O.; Palacio, H. A., 1994, Primary spacing evolution during directional solidification of Al-0.5 wt.% Cu, *Scripta Metallurgica et Materialia*, 31, p 1265.
- Fornaro, O.; Palacio, H. A., 1997, Planar to cellular transition during directional solidification of Al-0.5 wt.%Cu, *Scripta Materialia*, 36, p 439.
- Fornaro, O.; Palacio, H. A., 2006, Planar front instabilities during directional solidification of hcp: Zn-Cd dilute alloys, *Scripta Materialia*, 54, p2149.
- Fornaro, O.; Palacio, H. A. & Biloni, H., 2004, Characteristic substructures in directionally solidified dilute Al-Cu alloys, in *Solidification Processes and Microstructures. A Symposium in Honor of Prof. W. Kurz TMS Series Proc.*, p 219.
- Fornaro, O.; Palacio, H. A. & Biloni, H. 2006, Segregation substructures in dilute Al-Cu alloys directionally solidified, *Materials Science and Engineering A*, 417, p 134.
- Sekerka R. F., 1984, Morphological and hydrodynamic instabilities during phase transformations, *Physica D*, 12, p 212.